Environmental Science and Pollution Research (2018) 25:5474–5483
https://doi.org/10.1007/s11356-017-0862-9

RESEARCH ARTICLE

Amicarbazone degradation promoted by ZVI-activated persulfate: study of relevant variables for practical application

Cátia A. L. Graça[1] · Lucas T. N. Fugita[1] · Adriana Correia de Velosa[1] · Antonio Carlos S. C. Teixeira[1]

Received: 20 June 2017 / Accepted: 28 November 2017 / Published online: 7 December 2017
© Springer-Verlag GmbH Germany, part of Springer Nature 2017

Abstract

Alarming amounts of organic pollutants are being detected in waterbodies due to their ineffective removal by conventional treatment techniques, which warn of the urgent need of developing new technologies for their remediation. In this context, advanced oxidation processes (AOPs), especially those based on Fenton reactions, have proved to be suitable alternatives, due to their efficacy of removing persistent organic compounds. However, the use of ferrous iron in these processes has several operational constraints; to avoid this, an alternative iron source was here investigated: zero-valent-iron (ZVI). A Fenton-like process based on the activation of a recently explored oxidant-persulfate (PS)—with ZVI was applied to degrade an emerging contaminant: Amicarbazone (AMZ). The influence of ZVI size and source, PS/ZVI ratio, pH, UVA radiation, dissolved O_2, and inorganic ions was evaluated in terms of AMZ removal efficiency. So far, this is the first time these parameters are simultaneously investigated, in the same study, to evaluate a ZVI-activated PS process. The radical mechanism was also explored and two radical scavengers were used to determine the identity of major active species taking part in the degradation of AMZ. The degradation efficiency was found to be strongly affected by the ZVI dosage, while positively affected by the PS concentration. The PS/ZVI system enabled AMZ degradation in a wide range of pH, although with a lower efficiency under slightly alkaline conditions. Dissolved O_2 revealed to play an important role in reaction kinetics as well as the presence of inorganic ions. UVA radiation seems to improve the degradation kinetics only in the presence of extra O_2 content. Radicals quenching experiments indicated that both sulfate ($SO_4^{\bullet-}$) and hydroxyl ($^{\bullet}OH$) radicals contributed to the overall oxidation performance, but $SO_4^{\bullet-}$ was the dominant oxidative species.

Keywords Zero valent iron · Anions · UVA · Fenton-like processes · Sulfate-driven AOPs

Introduction

Advanced oxidation processes (AOPs) have received great attention as viable alternatives to degrade persistent organic contaminants not easily removed in conventional water and wastewater treatment processes (Oppenländer 2003; Stefan 2017). Fenton and Fenton-like processes, based on the reaction between a source of iron and a strong oxidant (e.g., H_2O_2), are among the most studied AOPs (Babuponnusami and Muthukumar 2014), and have proved to successfully degrade a large range of organic pollutants, such as pharmaceuticals (Trovó et al. 2009; Trovó et al. 2011), hormones (Xu et al. 2009), pesticides (Ma and Sung 2010; MacKul'Ak et al. 2011), and dyes (Sohrabi et al. 2014), among others. The so-called conventional AOPs are based on the production of hydroxyl radicals ($^{\bullet}OH$), which are powerful oxidizing species ($E_0 = 2.7$ V SHE) (Liang et al. 2007) that indiscriminately attack all the organic matter. However, lately, $SO_4^{\bullet-}$-driven AOPs have received growing attention due to their advantages as compared with $^{\bullet}OH$ -driven AOPs: the reactants used to generate $SO_4^{\bullet-}$ are cheaper and disperse in water for longer distances (considering the remediation of contaminated sites) (Zhang et al. 2014); $SO_4^{\bullet-}$ is less likely to be scavenged by non-target molecules (Ji et al. 2015) and will transform into sulfate ion subsequent to oxidation, which is considered

Responsible editor: Vítor Pais Vilar

Electronic supplementary material The online version of this article (https://doi.org/10.1007/s11356-017-0862-9) contains supplementary material, which is available to authorized users.

✉ Cátia A. L. Graça
catia.graca@usp.br

[1] Department of Chemical Engineering, University of São Paulo, Av. Prof. Luciano Gualberto, tr. 3, São Paulo 380, Brazil

environmentally friendly (Gao et al. 2012; Zhang et al. 2014). One of the most used reactants to generate $SO_4^{\bullet-}$ is persulfate ion ($S_2O_8^{2-}$), which can be activated by heat (Ji et al. 2015), base (Furman et al. 2010), UV radiation (Rasoulifard et al. 2012; Graça et al. 2017a), and transition metals (Liu et al. 2012). Similar to the Fenton process, iron as ferrous ion (Fe^{2+}) has been the metal most employed in PS activation (Eq. 1) because of its high abundance, low-cost, and non-toxic properties. Therefore, this technique can be considered a Fenton-like process.

$$Fe^{2+} + S_2O_8^{2-} \rightarrow 2SO_4^{\bullet-} + SO_4^{2-} + Fe^{3+} \quad (1)$$

However, when Fe^{2+} is oxidized to Fe^{3+}, the PS activation is halted; large amounts of Fe^{2+} are thus required to compensate this effect, which is a disadvantage of this process. This could also represent another drawback, since too much Fe^{2+} can scavenge sulfate radicals (Eq. 2), leading to a decline in the process efficiency (Han et al. 2015).

$$Fe^{2+} + SO_4^{\bullet-} \rightarrow Fe^{3+} + SO_4^{2-} \quad (2)$$

For these reasons, alternative sources of Fe^{2+} such as UVA irradiated magnetite (Avetta et al. 2015) and Fe(III)-complexes (Graça et al. 2017a) have been explored for a more efficient PS activation by means of Fe^{2+} recycling. In the absence of light, zero valent iron (ZVI) can also be used as an alternative way to induce PS activation by gradually releasing Fe^{2+} in water (Eqs. 3 and 4). This enables PS activation for extended periods (Deng et al. 2014) or by reacting directly on the surface of ZVI particles (Eq. 5) (Weng and Tao 2015).

$$2Fe^0 + O_2 + 2H_2O \rightarrow 2Fe^{2+} + 4OH^- \quad (3)$$

$$Fe^0 + 2H_2O \rightarrow Fe^{2+} + 2OH^- + H_2 \quad (4)$$

$$S_2O_8^{2-} + Fe^0(s) \rightarrow Fe^{2+} + 2SO_4^{\bullet-} + 2e^- \quad (5)$$

ZVI has already shown to be more effective than Fe^{2+} or Fe^{3+} in PS activation for a wider range of pH (Deng et al. 2014), being, therefore, more suitable for environmental applications. Modifications on ZVI particles with the aim of increasing their reaction effectiveness have been the target of many researches in recent years. For example, particles reactivity can be increased by increasing their surface area, thus nano-sized ZVI (nZVI) is expected to provide faster reactions when compared to granular ZVI (Fu et al. 2014). In fact, Li et al. (2014) demonstrated that nZVI revealed a faster activation of persulfate than micro or milli-ZVI on acid orange 7 degradation. We also evaluated the effectiveness of a ZVI-activated persulfate system in the degradation of an emerging pollutant: the herbicide amicarbazone (AMZ), widely applied in sugarcane and other cultivations. Over the last years, our group has been investigating AMZ fate and treatability: Peixoto and Teixeira (2014) studied AMZ UVC photolysis along with biodegradability essays, concluding that neither this herbicide nor its photolysis products are likely to be removed by conventional biological treatment processes. Silva et al. (2015) studied the sunlight-driven AMZ environmental fate, finding herbicide half-life times up to 75 days depending on surface water characteristics. Moreover, due to its extensive use and high water solubility (4.6 g L^{-1}), AMZ can easily contaminate either groundwater or surface waterbodies by leaching and runoff processes (Possamai et al. 2013). Based on this information, there is a high chance of this herbicide to become a regular contaminant of waterbodies near crop fields where it is frequently applied. Actually, there is already a study reporting AMZ contamination in Brazilian groundwater (Santos and Correia 2015), although under quantifiable levels.

Besides, this is a particularly interesting contaminant to study due to the existence of few records in the literature regarding its degradation by different AOP technologies (Peixoto and Teixeira 2014; Silva et al. 2015; Conceição et al. 2017; Graça et al. 2017a). Given that, our present research intents to contribute to the development of alternative techniques capable of degrading such contaminant. For that, in this study we investigated the effects of relevant variables for practical applications of the PS/ZVI process, namely, ZVI size and source, PS and ZVI initial concentration, pH, UVA radiation, and the presence of inorganic ions. To the best of our knowledge, literature discussing all these variables in the same study is inexistent; hence, our work brings an original contribution to the AOP state-of-the-art.

Materials and methods

Chemicals

Technical (> 95.4% m/m) and analytical grade (99.9% m/m) samples of amicarbazone were obtained from Arysta LifeScience Corp. and were used with no further purification. All the aqueous solutions were prepared in deionized water (18.2 MΩ cm), directly obtained from a Milli-Q Direct-Q system (Millipore). To test the influence of inorganic ions, samples of bottled mineral water (Baviera São Lourenço) were used as acquired and presented the following composition as reported by the bottle label: HCO_3^-, 42.82 mg L^{-1}; Sr^{2+}, 0.088 mg L^{-1}; Ca^{2+}, 1.960 mg L^{-1}; Mg^{2+}, 2.909 mg L^{-1}, K^+, 2.909 mg L^{-1}; Na^+, 11.500 mg L^{-1}, PO_4^{3-}, 0.11 mg L^{-1}; NO_3^-, 0.80 mg L^{-1}; Cl^-, 1.95 mg L^{-1}; SO_4^{2-}, 6.06 mg L^{-1}; F^-, 0.22 mg L^{-1}; Br^-, 0.03 mg L^{-1}; pH 7.03.

Commercial nano-scale ZVI particles (nZVI, NANOFER 25) were obtained from NANO IRON (Czech Republic) and used as received. According to the information provided by the manufacturer, these particles have a surface area of 20–25 m^2 g^{-1} and an average size of 50 nm. Other nZVI nanoparticles were prepared by the reducing ferrous iron using

sodium borohydride (98% purity), according to the procedure of Ponder et al. (2000). After synthesis, the nanoparticles were stored refrigerated in nitrogen-saturated water slurry (5% *w*/*v*) for at most 1 week. The sizes of individual particles were determined by Field Emission Gun-Scanning Electron Microscopy analysis (FEG-SEM) using a FEI Quanta 400 model.

Micro-scale ZVI particles were from J.T. Baker (USA). The surface area of these particles was 3.092 $m^2\ g^{-1}$ (determined by N_2 adsorption by a BET technique using a Micromeritics ASAP 2020 surface analyzer). All the other chemicals were of analytical grade.

Experimental procedures

All the experiments were carried out in duplicate in a 250-mL capacity beaker inside a closed container to avoid the influence of external light. The solution was kept under magnetic stirring to provide a constant mixing state. The reaction temperature was kept under 20 °C using a cool water bath to ensure that persulfate was not activated by heat. Firstly, the desired amount of ZVI was added to a 100-mL solution containing 41.4 μmol L^{-1} of AMZ. Although this concentration is possibly higher than that detected in the environment, it was chosen to allow its detection by our analytical apparatus during the degradation process. Then, PS was introduced to start the oxidation reaction. Sample aliquots (0.45 mL) were taken at specified times, were immediately filtered through 0.22-μm PVDF membranes to separate the ZVI particles from the reaction solution, and were mixed with 500 μL of MeOH to stop the reaction. In pH-controlled experiments, the pH was adjusted with NaOH or $HClO_4$ solutions. In UVA-irradiated experiments, the beaker containing the reaction solution was placed under four 15-W blacklight lamps (Sylvania F15 W/350 BL T8), positioned inside the closed container at 27 cm from the beaker and emitting 23.3 W m^{-2} in the wavelength range of 315–400 nm, as determined using a spectroradiometer (SPR 4002, Luzchem). To study the influence of dissolved oxygen, a stream of O_2 or N_2 was bubbled into the solution.

Analytical methods

Dissolved Fe(II) concentration was determined according to the o-phenantroline standardized procedure (Mortatti et al. 1982), and the red complex formed was determined spectrophotometrically at 510 nm using a Varian Cary 50 UV-Vis spectrophotometer.

AMZ concentration during the degradation experiments was followed by HPLC-UV (Shimadzu, Series 20A) using a C18 column (ACE, 250 mm × 4.6 mm, 5 μm). The isocratic elution procedure used 50% methanol and 50% of an aqueous solution containing 1% acetic acid, at a flow rate of 1.0 mL min^{-1}. The injection volume was 50 μL, and the detection wavelength was 230 nm. The limits of detection (LOD) and quantification (LOQ) were 1.03 and 3.09 μmol L^{-1}, respectively.

Results and discussion

nZVI characterization

The FEG-SEM analysis reveals that synthesized nZVI particles are spherical with diameters ranging from 103 to 582 nm (average 180 nm), and some aggregates larger than 1 μm (see Supplementary Information, Figure S1), which is in accordance with previous studies in which nZVI were synthesized by similar methods (Correia de Velosa and Pupo Nogueira 2013).

Influence of ZVI source and size

The influence of ZVI source and size on AMZ (41.4 μmol L^{-1}) degradation by PS/ZVI (1:1 mmol L^{-1}) is illustrated in Fig. 1a. Control experiments in the presence of either ZVI or PS alone were carried out varying the concentration of each reactant. No significant AMZ degradation was observed for 24 h, confirming that none of these reactants alone is responsible for the degradation observed over the reaction time (180 min maximum). As observed in Fig. 1, when PS and ZVI are mixed, they promote AMZ degradation, despite promoting distinct degradation profiles: nano-sized particles promoted a two-stage degradation, characterized by a faster one when PS and nZVI are mixed, followed by a stagnation phase, while micro-sized ZVI promoted gradual degradation over time.

As observed in Fig. 1b, a high amount of Fe(II) is released from nano-sized ZVI when it is mixed with PS, which could lead to the total PS consumption, not leaving enough for subsequent reaction. This explains the AMZ degradation profile promoted by these particles. Although synthesized nZVI continues to release Fe(II) up to 30 min, no further degradation is observed along this period, probably due to the scavenging effect of excessive Fe(II) (Eq. 2). On the other hand, Fig. 1b reveals a gradual Fe(II) release from micro-sized ZVI, which leads to a constant PS activation over time (Eq. 1), explaining the continuous AMZ degradation promoted by these particles.

One of the major advantages of using ZVI instead of dissolved Fe(II) to activate persulfate is the ability of the former to continuously activate PS over time, along with a gradual Fe(II) release, which was only observed with micro-sized ZVI. This result differs from what is normally reported, since smaller particles, due to their higher surface areas, generally lead to a higher PS activation due to higher Fe(II) release. However, this can be justified by the low PS concentration used in our experiments. Similarly, Li et al. (2014) verified no

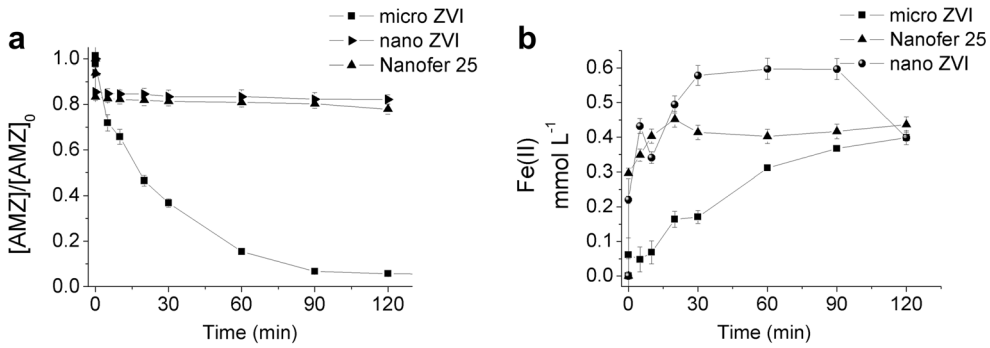

Fig. 1 **a** Influence of ZVI source and size on AMZ degradation by the PS/ZVI system (1:1). **b** Fe(II) released from PS/ZVI (1:1) experiments with micro ZVI, Nanofer 25, and nano ZVI, respectively. $[AMZ]_0 = (41.4 \pm 8)$ μmol L^{-1}; $[ZVI]_0 =$ 1 mmol L^{-1}; $[PS]_0 = 1$ mmol L^{-1}; free pH; $pH_0 \approx 3$

further mineralization of acid orange 7 after PS exhaustion due to an excessive Fe^{2+} release from nZVI at the beginning of reaction.

An interesting fact that also turns micro ZVI more attractive than nZVI for practical application is that nZVI of extremely small sizes can pose a threat to living organisms, given their capacity of entering cell membrane and cause damages (Phenrat et al. 2009). Despite the lack of literature concerning nZVI toxicity, this is something to keep aware whenever handling nanoparticles (Stefaniuk et al. 2016).

Nonetheless, in our experiments, micro ZVI was preferred to nZVI for PS activation to perform further ZVI/PS investigations, given its better performance.

Effect of initial ZVI and PS concentration

The effect of initial ZVI concentration was investigated by adding different amounts of micro ZVI into a 41.4 μmol L^{-1} (10 mg L^{-1}) AMZ solution, while the initial PS concentration was fixed at 1 mmol L^{-1}.

With no pH adjustment, a gradual pH increase was observed over time which is dependent on the initial ZVI concentration. The pH began to increase earlier (initial pH around 3 for all the experiments) for higher initial ZVI concentrations as expected, since the amount of OH^- anions released from iron corrosion is proportional to the initial Fe^0 concentration (Eqs. 3 and 4) (Deng et al. 2014). However, by the time pH increases (Fig. 2a), Fe^{2+} is no longer available to react with PS (Eq. 1) (Fig. 2b), since it is removed by precipitation, and AMZ degradation slows down as a consequence. This is more evident for a ZVI concentration of 20 mmol L^{-1}, for which Fe(II) measurements reveal a significant decrease after 30 min of reaction. Figure 2c allows observing that this slower AMZ degradation stage was reached earlier for higher ZVI initial concentrations, which consequently led to less AMZ removals for equal degradation periods. In the same way, AMZ degradation followed a pseudo first-order behavior for shorter times as the ZVI concentration increased. To facilitate comparison between kinetics, the observed degradation rate constants (k_{obs}) were all calculated up to 30 min of reaction, giving the following values: of 3.13×10^{-2} min^{-1} for PS/ZVI ratio 1:1, 4.0×10^{-2} min^{-1} for PS/ZVI ratio 1:5 and 1:10 and 3.02×10^{-3} min^{-1} for PS/ZVI ratio 1:20. Another factor that may have contributed to less AMZ removals as the ZVI concentration increased above 10 mmol L^{-1} was $SO_4^{\bullet-}$ scavenging by excessive amounts of Fe^{2+} (Eq. 2), thereby reducing the degradation efficiency. This feature is supported by Fe(II) measurements shown in Fig. 2b, since the initial Fe(II) release increases when the ZVI concentration is increased. Similar results were observed by Wei et al. (2016), who reported that high amounts of ZVI decreased the PS/ZVI efficiency in bentazon degradation due to sulfate radicals scavenging by excessive Fe(II).

Conversely, the effect of initial PS concentration was investigated by spiking different amounts of PS into a 41.4 μmol L^{-1} AMZ solution, while the initial ZVI concentration was fixed at 5 mmol L^{-1}. As expected, AMZ degradation increased by increasing the PS initial concentration (Fig. 3a), since more radicals were expected to be generated. Also, higher initial PS concentration kept a lower pH over the reaction time, since increasing persulfate ions in aqueous solution increased H^+ release (Eqs. 7 and 8) (Ghauch et al. 2013). As a consequence, more $SO_4^{\bullet-}$ radicals would be produced, since the formation and maintenance of ferrous ions (Fe^{2+}) in solution (Eq. 6) is favored under acidic conditions (Fig. 3b) (Wei et al. 2016), therefore more Fe^{2+} is available to react with PS. Also, it is clear in Fig. 3b that Fe(II) measurements up to 30 min decrease with increasing PS concentration, suggesting that, during this period, Fe(II) consumption is higher than its production, which explains the increasing AMZ degradation. After that, a stagnation phase appears, probably due to excessive Fe(II) or to a high PS consumption. In this case, k_{obs} values of 1.5×10^{-2} min^{-1} and 7.7×10^{-2} min^{-1} were obtained for PS/ZVI ratios of 0.5:5 and 2.5:5, respectively (both calculated based on data up to 30 min of reaction).

$$Fe^0 + 2H^+ \rightarrow Fe^{2+} + H_2 \quad (6)$$

$$2S_2O_8^{2-} + 2H_2O \rightarrow 4HSO_4^- + O_2 \quad (7)$$

$$HSO_4^- \rightarrow SO_4^{2-} + H^+ \quad (8)$$

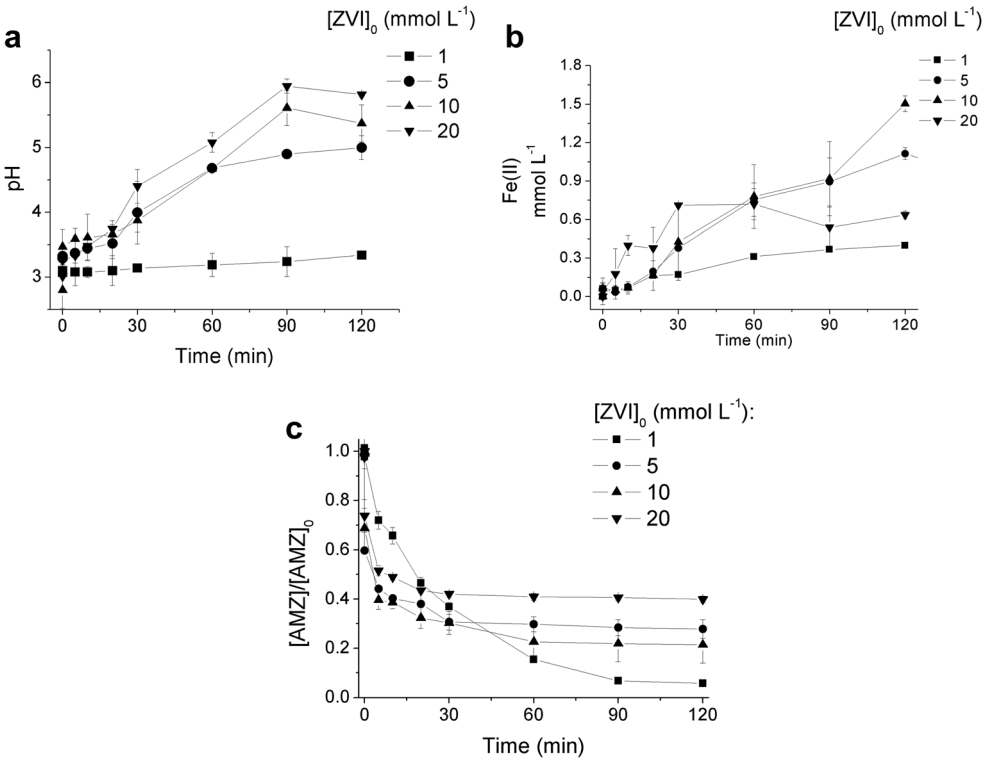

Fig. 2 Effect of $[ZVI]_0$ on **a** pH profile over reaction **b** Fe^{2+} release during reaction. **c** AMZ degradation by the PS/ZVI system. $[AMZ]_0 = (41.4 \pm 8.0)$ μmol L^{-1}; $[PS]_0 =$ 1 mmol L^{-1}; $1 < [ZVI]_0 <$ 20 mmol L^{-1}; free pH, $pH_0 \sim 3$

The two PS/ZVI ratios that promoted the highest AMZ removal, i.e., 1:1 and 2.5:5, where chosen to perform the experiments described in the subsequent sections. Previous studies in which the PS/ZVI system was applied to oxidize organic pollutants, namely, acetaminophen and polyvinyl alcohol, also reported a PS/ZVI molar ratio of 1:1 as the optimum (Oh et al. 2009; Deng et al. 2014).

Effect of solution pH

To evaluate the effect of pH on AMZ degradation, experiments were carried out at three different pH: 3.5, 5, and 8. The effect of pH on AMZ degradation promoted by the PS/ZVI process for PS/ZVI ratios of 1:1 and 2.5:5 is shown in Fig. 4a, b, respectively. The PS/ZVI system promoted AMZ degradation over a broad pH range, although with a slower rate at pH 8. This happened because iron ions are insoluble at such pH, forming precipitates. Even so, for the higher PS/ZVI ratio, almost 70% AMZ removal was achieved under alkaline conditions, indicating that higher loads of ZVI and PS together can overcome this drawback. One of the reasons behind this behavior can rely on the generation of sulfate radicals via the surface reaction (Eq. 5) even under slightly alkaline conditions (Weng and Tao 2015). Another reason is the possibility of generating stronger oxidizing radicals, such as hydroxyl radical under alkaline media (Eq. 9):

$$SO_4^{\bullet-} + SO^- \rightarrow SO_4^{2-} + {}^{\bullet}OH \quad (9)$$

However, it is possible to observe that, for both ratios, at pH 8, the degradation rate starts declining after a certain time. This feature can be attributed to the absence of corrosion

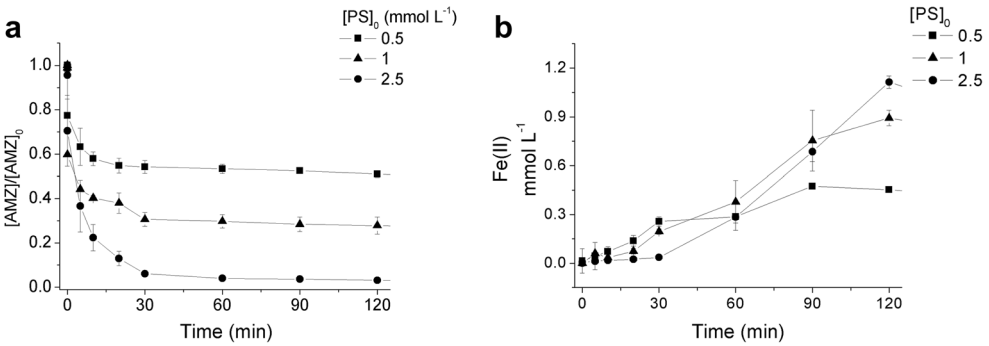

Fig. 3 Effect of [PS]0 on **a** AMZ degradation and **b** Fe2+ concentrations at the end of 120 min of reaction. $[AMZ]0 = (41.4 \pm 8.0)$ μmol L^{-1}; $[ZVI]0 = 5$ mmol L^{-1}; $0.5 < [PS]0 < 2.5$ mmol L^{-1}; free pH. pH $0 \sim 3$

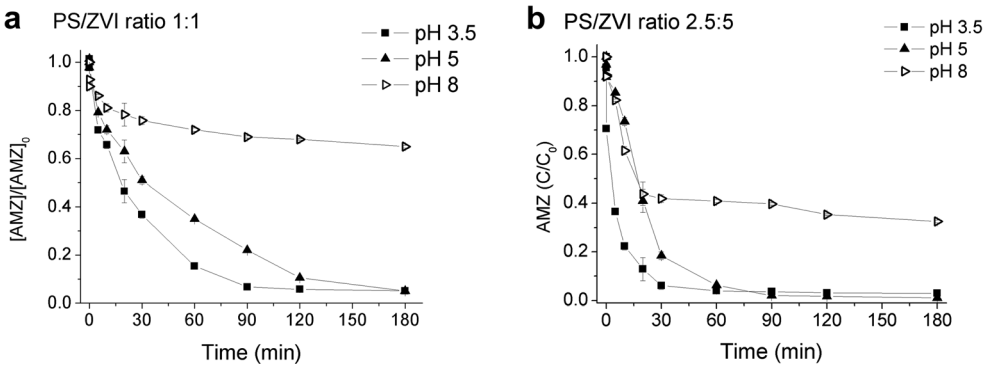

Fig. 4 Effect of solution pH on AMZ degradation by the PS/ZVI system, for PS/ZVI ratios of **a** 1:1 and **b** 2.5:5. $[AMZ]_0 = (41.4 \pm 8)$ μmol L^{-1}

under these circumstances, therefore not providing new active sites that could be available in deeper layers of the ZVI particle. Decreasing the number of active sites on the ZVI surface, decreases the chance of PS to react via the surface reaction (Eq. 5).

Under acidic conditions, both ratios enabled AMZ removals below LOQ after 120 min of reaction, indicating that lower pH values are better for such processes, as expected, given the highest Fe^{2+} release.

Studies in which dissolved Fe^{2+}–activated PS was applied to degrade organic pollutants reported that this process is only effective under acidic conditions (Cao et al. 2008; Rao et al. 2014). Given that, our results confirm that ZVI is a much more suitable PS activator than Fe^{2+}, since it allows working in a wider pH range.

Influence of UVA radiation

The presence of iron species in surface waters exposed to sunlight is known to contribute to the auto-depuration of water bodies (Cieśla et al. 2004; Graça et al. 2017b). Therefore, it is worth assessing the behavior of the PS/ZVI system on AMZ degradation in the presence of UVA radiation, which is the UV radiation most incident on the Earth's surface (300–400 nm). The influence of UVA radiation on AMZ degradation by the PS/ZVI system for both PS/ZVI ratios tested is presented in Fig. 5. As observed, the presence of UVA slightly enhanced AMZ degradation only in the PS/ZVI ratio of 2.5:5, although no significant differences were observed between degradation rates, for both ratios (k_{obs} $(1:1)_{UVA} = 2.1 \times 10^{-2}$, k_{obs} $(1:1)_{dark} = 3.1 \times 10^{-2}$, k_{obs} $(2.5:5)_{UVA} = 14 \times 10^{-2}$, k_{obs} $(2.5:5)_{dark} = 9.2 \times 10^{-2}$). As explored in our previous investigation, the advantages of using UVA radiation on Fe^{2+}/PS systems rely on the generation of extra radicals from UVA-activated PS (Eq. 10) as well as from the photolysis of Fe^{3+}-aquacomplexes (Eq. 11). These promote Fe(II) recycling, thus extending the reaction described in Eq. 1 (Graça et al. 2017a). However, there are evidences in the literature revealing that excess $SO_4^{\bullet-}$ in the PS/ZVI system can actually scavenge $SO_4^{\bullet-}$ itself (Eq. 12) (Deng et al. 2014). Also, excess Fe^{2+} ions generated by the reactions given by Eqs. 11, 3, and 5 can scavenge sulfate radicals (Eq. 2). These scavenging side reactions would nullify the increment that extra radicals promote in AMZ degradation, possibly explaining the almost insignificant influence of UVA we observed. In fact, PS measurements (data not shown) confirm a higher consumption of this reactant in the presence of UVA, thus suggesting that more sulfate radicals should have been generated. However, our results indicate that the PS/ZVI process would still be effective in AMZ degradation in surface waters exposed to sunlight, since high percentages of AMZ removal were achieved under UVA radiation.

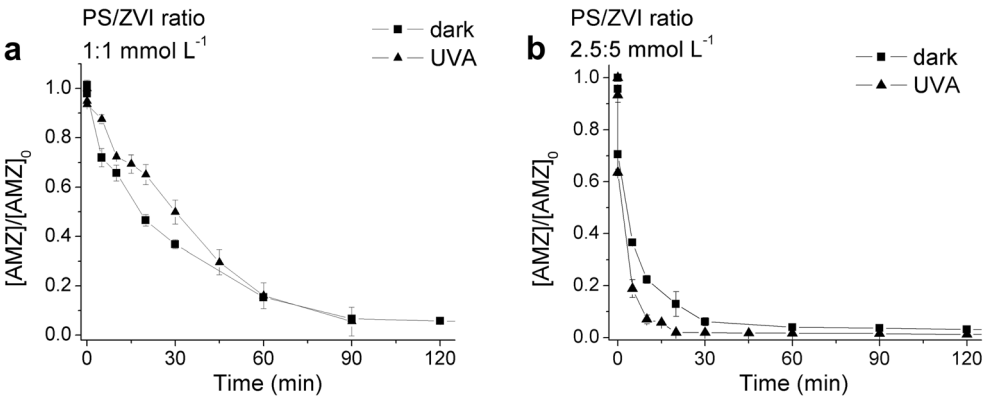

Fig. 5 Influence of UVA radiation on AMZ degradation by the PS/ZVI system for PS/ZVI ratios of **a** 1:1 and **b** 2.5:5. $[AMZ]_0 = (41.4 \pm 8)$ μmol L^{-1}, free pH. $pH_0 \approx 3$

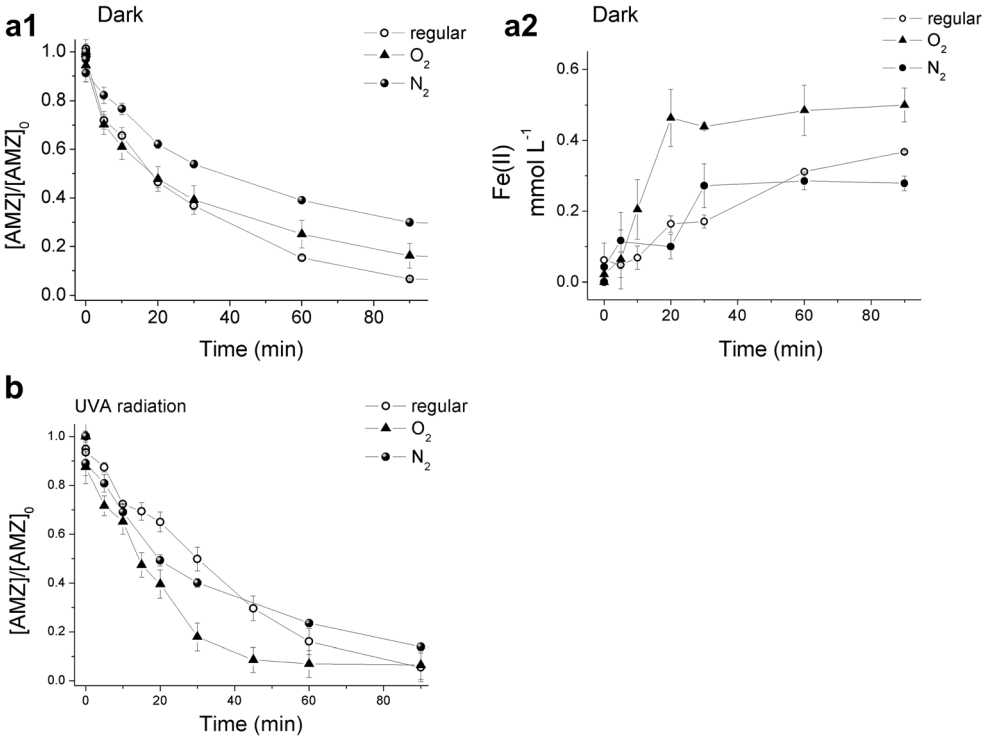

Fig. 6 **a1** Influence of dissolved oxygen on AMZ degradation by the PS/ZVI system (1:1 mmol L^{-1}) in the dark or **b** in the presence of UVA radiation. **a2** Influence of dissolved oxygen on released Fe(II) during AMZ degradation in the dark;$[AMZ]_0 = (41.4 \pm 8)$ μmol L^{-1}, free pH, $pH_0 \approx 3$

$$S_2O_8^{2-} + UV \rightarrow 2SO_4^{\bullet -} \quad (10)$$

$$\left[Fe^{III}OH(H_2O)_5\right]^{2+} + H_2O \xrightarrow{h\upsilon(LMCT)} \left[Fe^{II}(H_2O)_6\right]^{2+} + {}^{\bullet}OH \quad (11)$$

$$SO_4^{\bullet -} + SO_4^{\bullet -} \rightarrow S_2O_8^{2-} \quad (12)$$

Influence of dissolved oxygen

The influence of dissolved oxygen was studied here by bubbling high purity O_2 or N_2 gas in the reaction medium, for the PS/ZVI ratio of 1:1, in the absence or presence of UVA radiation (Fig. 6). As shown in Figure 6a1, increasing the content of dissolved oxygen in solution in the dark leads to a slight decrease on AMZ removal after 30 min of reaction, while decreasing the O_2 content by bubbling N_2 clearly inhibited AMZ removal. By bubbling O_2, the ZVI corrosion increases, resulting not only in a higher Fe(II) release (see Figure 6A2) but also in a faster pH increase (from 3 to 5 in 30 min) (Eq. 3) and oxidation of Fe(II) to Fe(III), which can explain the slower AMZ degradation rate after 30 min of reaction. On the other hand, when N_2 is purged into solution the same quantity of Fe(II) is generated but a lower AMZ degradation is verified.

Oxygen is known to play an important role in free radicals chemistry and in the degradation of organic compounds. Once hydroxyl or sulfate radicals initiate the free radical reaction by abstracting a hydrogen atom, molecular oxygen reacts with the carbon radical ($R^{\bullet}$) (scheme 1) to generate peroxyl radicals that can propagate the free radical chain reaction either by hydrogen abstraction or by generating excited species, such as triplet carbonyls or singlet oxygen, which are highly oxidant species (Eberhardt 2001).

However, in the presence of UVA radiation, the increase of dissolved O_2 content greatly enhanced AMZ degradation, while decreasing the O_2 concentration did not show any significant impact (Fig. 6B). In this case, the low effect of the absence of nitrogen in AMZ degradation is probably compensated by the production of extra sulfate radicals by the UVA-activated PS. On the other hand, increasing O_2 concentration in the irradiated system has a greater impact than in the dark, since irradiation provides extra radicals, not only via UVA-activated persulfate but also via Fe(III)-Fe(II) recycling (Eq. 11), extending the reaction described by Eq. 2.

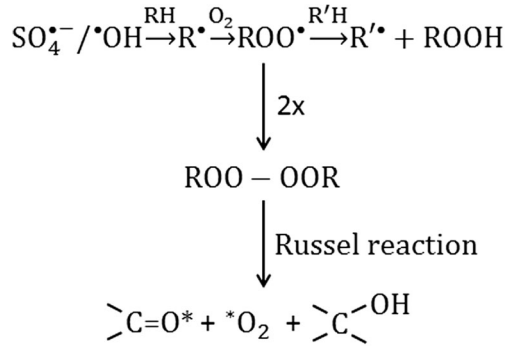

Scheme 1 Oxygen role on free radicals initiated reactions

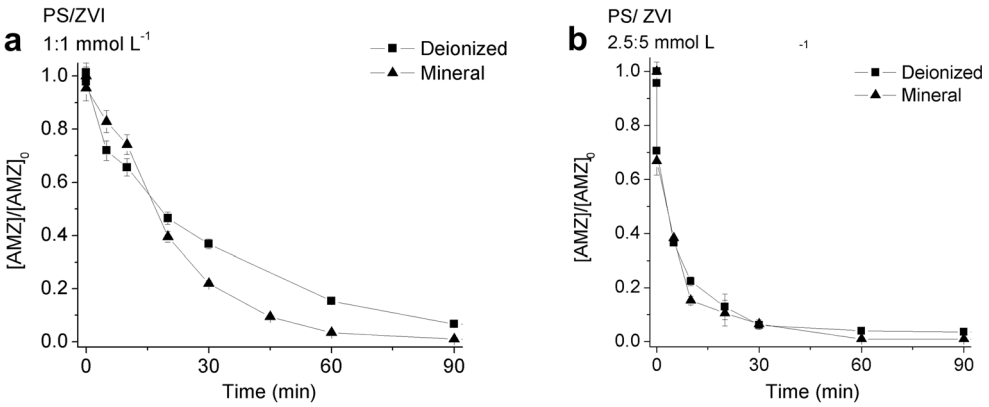

Fig. 7 Influence of different water matrices on AMZ degradation by the PS/ZVI system, for PS/ZVI ratios of **a** 1:1 and **b** 2.5/5. $[AMZ]_0 = (41.4 \pm 8)$ μmol L^{-1}, free pH, $pH_0 \approx 3$

Influence of inorganic constituents of natural waters

To study the effect of several inorganic ions usually present in natural waters on the performance of the PS/ZVI system used to degrade AMZ, experiments were performed using bottled mineral water instead of deionized water. Both PS/ZVI ratios (1:1 and 2.5:5 M ratios) were tested. Figure 7 shows that, for both PS/ZVI ratios, the degradation of AMZ in mineral water was slightly faster than that observed in deionized water. The mineral water used in our experiments is rich in HCO_3^- and SO_4^{2-} anions, well-known radical scavengers (Ghauch et al. 2013; Li et al. 2015); therefore, our results are in opposition to what is usually reported. Nonetheless, differing results like ours have already been reported in the literature. For instance, Velosa and Nascimento (2017) also reported similar results for sulfathiazole degradation present in a Sewage Treatment Plant effluent promoted by activated persulfate. Furthermore, there are already evidences in the literature mentioning that the addition of carbonates to activated-persulfate systems can generate reactive carbonate species capable of catalyzing the propagation reactions, resulting in more sulfate radicals (Bennedsen et al. 2012), which would explain the higher AMZ degradation observed in mineral water. In addition, although not observed in our experiments, salts are known to increase the rate of iron corrosion (Zakowski et al. 2014), due to an increase in water conductivity, leading to a higher Fe^{2+} release from ZVI particles, and more $SO_4^{\bullet-}$ production from the reaction between the latter and PS (Eq. 1), as a consequence. Given that, our results indicate that the PS/ZVI system is an attractive alternative for treating (i) groundwater contaminated with AMZ with on-site active barriers or by pumping and treating off-site; (ii) contaminated rinsing water generated in land farm use, particularly from spray equipment and containers, water used to wash vegetables and fruits, etc.; and (iii) contaminated water from plastic bottles (containing pesticide) washing prior to crushing and pelletization in plastic container recycling operations.

Identification of active radicals

As already mentioned, both $^{\bullet}OH$ and $SO_4^{\bullet-}$ radicals can be simultaneously produced in the studied system, be it in the absence or presence of UVA radiation. In order to identify the predominant oxidative species for both PS/ZVI ratios, in the absence or presence of light, 2-propanol and tert-butyl alcohol (TBA) were used as radical probes to weigh the contributions of $SO_4^{\bullet-}$ and $^{\bullet}OH$ species to the herbicide removal. These two specific alcohols were chosen because 2-propanol can scavenge both $^{\bullet}OH$ and $SO_4^{\bullet-}$ with very high rate constants, i.e., 1.9×10^9 L mol^{-1} s^{-1} and 4×10^7 L mol^{-1} s^{-1} (Buxton et al. 1988; Neta et al. 1988), respectively, while TBA is an effective quencher for $^{\bullet}OH$ ($k = 3.8–7.6 \times 10^8$ L mol^{-1} s^{-1}) but not for $SO_4^{\bullet-}$ ($k = 4–9.1 \times 10^5$ L mol^{-1} s^{-1}) (Han et al. 2015). To perform these experiments, two different probe/AMZ proportions were used: 500/1 and 1000/1 (molar ratios) and AMZ degradation was followed over the first 90 min of reaction. The results in Table 1 show that 2-propanol dramatically inhibited AMZ degradation for both PS/ZVI ratios, with or without UVA radiation, whereas TBA also suppressed AMZ, yet to a lesser

Table 1 Effect of 2-propanol and TBA on AMZ degradation by the PS/ZVI system, for PS/ZVI ratios of 1:1 and 2.5:5 (mmol L^{-1}), in the absence and in the presence of UVA radiation

	PS/ZVI ratio	AMZ removal (%) in 90 min of reaction				
		Without quencher	2-propanol		TBA	
			500/1	1000/1	500/1	1000/1
Without UVA	1:1	94.8	19	5	29	44
	2.5:5	97	30	15	97	50
With UVA	1:1	94.5	8	10	60	77
	2.5:5	98.8	28	13	93	98.8

extent, except for the PS/ZVI ratio 2.5:5 without UVA irradiation. These results indicate that both $^{\bullet}OH$ and $SO_4^{\bullet-}$ contributed to the overall removal of AMZ, although $SO_4^{\bullet-}$ radicals clearly play a more important role. In the case in which TBA inhibited AMZ degradation to a greater extent, probably more $^{\bullet}OH$ radicals were participating, since less PS was used (1 mmol L^{-1}) and, in the absence of UVA radiation, an early pH increase occurred, which might have led to more radical interconversion (Eq. 9) than in any other case.

Conclusions

In this study, the suitability of ZVI as a PS activator for degrading the herbicide amicarbazone (AMZ) was investigated. The effects of variables such as ZVI size, PS/ZVI ratio, suspension pH, dissolved oxygen content, UVA radiation, and presence of inorganic ions on the PS/ZVI system were evaluated in terms of AMZ removal. Our results indicated that micro-sized iron performed better than the two other nano-sized iron sources, and that increasing its concentration above 10 mmol L^{-1} negatively affected the PS/ZVI system. However, this negative effect can be surpassed by increasing the PS concentration. Slightly alkaline conditions were found not to be the most adequate for the PS/ZVI system, although significant AMZ removals were still possible under such conditions, with a high PS/ZVI ratio, which revealed to be an advantage of using a solid iron source. The incidence of UVA radiation alone did not seem to significantly affect the PS/ZVI system, but together with a higher content of dissolved oxygen, it boosts AMZ degradation. Even in the absence of light, oxygen was proved to play an important role in this process. Contrary to what is usually reported, the presence of inorganic ions revealed to slightly enhance AMZ degradation, which can be attributed to the catalyzed sulfate radical production by carbonate reactive species. Tests with radical scavengers confirmed that the major active species taking part in the process studied is the sulfate radical. Given that, our research demonstrates that ZVI can be an effective alternative to PS activation applied for water decontamination purposes.

Acknowledgements The authors would like to thank Taniele Araújo (from UFRN, Brazil) for her help in some experiments, as well as BE Mundus organization, FAPESP (grant nos. 2013/50218-2, 2013/09543-7, 2013/04656-8) and CAPES-PROCAD (grant 88881.068433/2014-01) for the financial support.

References

Avetta P, Pensato A, Minella M, Malandrino M, Maurino V, Minero C, Hanna K, Vione D (2015) Activation of persulfate by irradiated magnetite: implications for the degradation of phenol under heterogeneous photo-fenton-like conditions. Environ Sci Technol 49(2):1043–1050. https://doi.org/10.1021/es503741d

Babuponnusami A, Muthukumar K (2014) A review on Fenton and improvements to the Fenton process for wastewater treatment. J Environ Chem Eng 2(1):557–572. https://doi.org/10.1016/j.jece.2013.10.011

Bennedsen LR, Muff J, Søgaard EG (2012) Influence of chloride and carbonates on the reactivity of activated persulfate. Chemosphere 86(11):1092–1097. https://doi.org/10.1016/j.chemosphere.2011.12.011

Buxton GV, Greenstock CL, Helman WP, Ross AB (1988) Critical review of rate constants for reactions of hydrated electrons, hydrogen atoms and hydroxyl radicals (OH/O^-) in aqueous solution. J Phys Chem Ref Data 17(2):513–886. https://doi.org/10.1063/1.555805

Cao JS, Zhang WX, Brown DG, Sethi D (2008) Oxidation of lindane with Fe(II)-activated sodium persulfate. Environ Eng Sci 25(2):221–228. https://doi.org/10.1089/ees.2006.0244

Cieśla P, Kocot P, Mytych P, Stasicka Z (2004) Homogeneous photocatalysis by transition metal complexes in the environment. J Mol Catal A Chem 224(1-2):17–33. https://doi.org/10.1016/j.molcata.2004.08.043

Conceição DS, Ferreira DP, Graça CAL, Júlio MF, Ilharco LM, Velosa AC, Santos PF, Vieira Ferreira LF (2017) Photochemical and photocatalytic evaluation of 1D titanate / TiO_2 based nanomaterials. Appl Surf Sci 392:418–429. https://doi.org/10.1016/j.apsusc.2016.09.067

Correia de Velosa A, Pupo Nogueira RF (2013) 2,4-Dichlorophenoxyacetic acid (2,4-D) degradation promoted by nanoparticulate zerovalent iron (nZVI) in aerobic suspensions. J Environ Manag 121:72–79. https://doi.org/10.1016/j.jenvman.2013.02.031

Deng J, Shao Y, Gao N, Deng Y, Tan C, Zhou S (2014) Zero-valent iron/persulfate(Fe^0/PS) oxidation acetaminophen in water. Int J Environ Sci Technol 11(4):881–890. https://doi.org/10.1007/s13762-013-0284-2

Eberhardt M (2001) Reactive oxygen metabolites. In: Chemistry and Medical Consequences. CRC Press, Boca Raton

Fu F, Dionysiou DD, Liu H (2014) The use of zero-valent iron for groundwater remediation and wastewater treatment: a review. J Hazard Mater 267:194–205. https://doi.org/10.1016/j.jhazmat.2013.12.062

Furman OS, Teel AL, Watts RJ (2010) Mechanism of base activation of persulfate. Environ Sci Technol 44(16):6423–6428. https://doi.org/10.1021/es1013714

Gao YQ, Gao NY, Deng Y et al (2012) Ultraviolet (UV) light-activated persulfate oxidation of sulfamethazine in water. Chem Eng J 195–196:248–253. https://doi.org/10.1016/j.cej.2012.04.084

Ghauch A, Ayoub G, Naim S (2013) Degradation of sulfamethoxazole by persulfate assisted micrometric Fe^0 in aqueous solution. Chem Eng J 228:1168–1181. https://doi.org/10.1016/j.cej.2013.05.045

Graça CAL, Velosa AC, Teixeira ACSC (2017a) Amicarbazone degradation by UVA-activated persulfate in the presence of hydrogen peroxide or Fe^{2+}. Catal Today 280:80–85. https://doi.org/10.1016/j.cattod.2016.06.044

Graça CAL, Velosa AC, Teixeira ACSC (2017b) Role of Fe(III)-carboxylates in AMZ photodegradation: a response surface study based on a Doehlert experimental design. Chemosphere 184:981–991. https://doi.org/10.1016/j.chemosphere.2017.06.013

Han D, Wan J, Ma Y, Wang Y, Li Y, Li D, Guan Z (2015) New insights into the role of organic chelating agents in Fe(II)-activated persulfate processes. Chem Eng J 269:425–433. https://doi.org/10.1016/j.cej.2015.01.106

Ji Y, Dong C, Kong D, Lu J, Zhou Q (2015) Heat-activated persulfate oxidation of atrazine: implications for remediation of groundwater contaminated by herbicides. Chem Eng J 263:45–54. https://doi.org/10.1016/j.cej.2014.10.097

Li H, Wan J, Ma Y, Wang Y, Huang M (2014) Influence of particle size of zero-valent iron and dissolved silica on the reactivity of activated persulfate for degradation of acid orange 7. Chem Eng J 237:487–496. https://doi.org/10.1016/j.cej.2013.10.035

Li H, Wan J, Ma Y, Wang Y, Guan Z (2015) Role of inorganic ions and dissolved natural organic matters on persulfate oxidation of acid orange 7 with zero-valent iron. RSC Adv 5(121):99935–99943. https://doi.org/10.1039/C5RA16094D

Liang C, Wang Z, Bruell CJ (2007) Influence of pH on persulfate oxidation of TCE at ambient temperatures. Chemosphere 66(1):106–113. https://doi.org/10.1016/j.chemosphere.2006.05.026

Liu CS, Shih K, Sun CX, Wang F (2012) Oxidative degradation of propachlor by ferrous and copper ion activated persulfate. Sci Total Environ 416:507–512. https://doi.org/10.1016/j.scitotenv.2011.12.004

Ma Y-S, Sung C-F (2010) Investigation of carbofuran decomposition by a combination of ultrasound and Fenton process. J Environ Eng Manag 20:213–219

MacKul'Ak T, Prousek J, Švorc L (2011) Degradation of atrazine by Fenton and modified Fenton reactions. Monatshefte fur Chemie 142(6):561–567. https://doi.org/10.1007/s00706-011-0504-8

Mortatti FJ, Krug LCR, Pessenda et al (1982) Determination of iron in natural waters and plant material with 1,10-phenanthroline by flow injection analysis. Analyst 107(659–6):659–663. https://doi.org/10.1039/AN9820700659

Neta P, Huie RE, Ross AB (1988) Rate constants for reaction of inorganic radicals in aqueous solution. J Phys Chem Ref Data 17:1027–1284

Oh SY, Kim HW, Park JM et al (2009) Oxidation of polyvinyl alcohol by persulfate activated with heat, Fe^{2+}, and zero-valent iron. J Hazard Mater 168(1):346–351. https://doi.org/10.1016/j.jhazmat.2009.02.065

Oppenländer T (2003) Photochemical purification of water and air: advanced oxidation processes (AOPs): principals, reaction mechanisms, reactor concepts. Wiley-VCH, Weinheim

Peixoto AL, Teixeira ACSC (2014) Degradation of amicarbazone herbicide by photochemical processes. J Photochem Photobiol A Chem 275:54–64. https://doi.org/10.1016/j.jphotochem.2013.10.013

Phenrat T, Long TC, Lowry GV (2009) Partial oxidation ("aging") and surface modification decrease the toxicity of nanosized zerovalent iron. Environ Sci Technol 43(1):195–200. https://doi.org/10.1021/es801955n

Ponder SM, Darab JG, Mallouk TE (2000) Remediation of Cr(VI) and Pb(II) aqueous solutions using supported, nanoscale zero-valent iron. Environ Sci Technol 34(12):2564–2569. https://doi.org/10.1021/es9911420

Possamai ACS, Inoue MH, Mendes KF, Santana DC, Ben R, Santos EG (2013) Leaching potential and residual effect of amicarbazone in soils of contrasting texture. Semin. Ciênc Agrar 34(5):2203–2210. https://doi.org/10.5433/1679-0359.2013v34n5p2203

Rao YF, Qu L, Yang H, Chu W (2014) Degradation of carbamazepine by Fe(II)-activated persulfate process. J Hazard Mater 268:23–32. https://doi.org/10.1016/j.jhazmat.2014.01.010

Rasoulifard M, Majidzadeh H, Demneh F, Babaei E (2012) Photocatalytic degradation of tylosin via ultraviolet-activated persulfate in aqueous solution. Int J Ind Chem 3(1):16. https://doi.org/10.1186/2228-5547-3-16

Santos EA, Correia NM (2015) Herbicide detection in groundwater in Córrego Rico-SP. Planta Daninha 33:147–155. https://doi.org/10.1590/S0100-83582015000100017

Silva MP, Mostafa S, McKay G, Rosario-Ortiz FL, Teixeira ACSC (2015) Photochemical fate of amicarbazone in aqueous media: laboratory measurement and simulations. Environ Eng Sci 32(8):1–11. https://doi.org/10.1089/ees.2015.0127

Sohrabi MR, Khavaran A, Shariati S, Shariati S (2014) Removal of Carmoisine edible dye by Fenton and photo Fenton processes using Taguchi orthogonal array design. Arab J Chem 10:S3523–S3531. https://doi.org/10.1016/j.arabjc.2014.02.019

Stefan MI (ed) (2017) Advanced oxidation processes for water treatment: fundamentals and applications. IWA publishing, London

Stefaniuk M, Oleszczuk P, Ok Y (2016) Review on nano zerovalent iron (nZVI): from modification to environmental applications. Chem Eng J 287:618–632. https://doi.org/10.1016/j.cej.2015.11.046

Trovó AG, Nogueira RFP, Agüera A, Fernandez-Alba AR, Sirtori C, Malato S (2009) Degradation of sulfamethoxazole in water by solar photo-Fenton. Chemical and toxicological evaluation. Water Res 43(16):3922–3931. https://doi.org/10.1016/j.watres.2009.04.006

Trovó AG, Pupo Nogueira RF, Aguera A et al (2011) Degradation of the antibiotic amoxicillin by photo-Fenton process - chemical and toxicological assessment. Water Res 45(3):1394–1402. https://doi.org/10.1016/j.watres.2010.10.029

Velosa AC, Nascimento CAO (2017) Evaluation of sulfathiazole degradation by persulfate in Milli-Q water and in effluent of a sewage treatment plant. Environ Sci Pollut Res 24(7):6270–6277. https://doi.org/10.1007/s11356-016-7036-z

Wei X, Gao N, Li C, Deng Y, Zhou S, Li L (2016) Zero-valent iron (ZVI) activation of persulfate (PS) for oxidation of bentazon in water. Chem Eng J 285:660–670. https://doi.org/10.1016/j.cej.2015.08.120

Weng C, Tao H (2015) Highly efficient persulfate oxidation process activated with Fe^0 aggregate for decolorization of reactive azo dye Remazol golden yellow. Arab J Chem. https://doi.org/10.1016/j.arabjc.2015.05.012

Xu XR, Li XY, Li XZ, Bin LH (2009) Degradation of melatonin by UV, UV/H_2O_2, Fe^{2+}/H_2O_2 and $UV/Fe^{2+}/H_2O_2$ processes. Sep Purif Technol 68(2):261–266. https://doi.org/10.1016/j.seppur.2009.05.013

Zakowski K, Narozny M, Szocinski M (2014) Influence of water salinity on corrosion risk — the case of the southern Baltic Sea coast. Environ Monit Assess 186(8):4871–4879. https://doi.org/10.1007/s10661-014-3744-3

Zhang Q, Chen J, Dai C, Zhang Y, Zhou X (2014) Degradation of carbamazepine and toxicity evaluation using the UV/persulfate process in aqueous solution. J Chem Technol Biotechnol 90(4):701–708. https://doi.org/10.1002/jctb.4360